Laboratory Investigation (2010) 90, 577–588

Long-term bacterial exposure can trigger nonsuppurative destructive cholangitis associated with multifocal epithelial inflammation

Ikuko Haruta[1], Ken Kikuchi[2], Etsuko Hashimoto[3], Minoru Nakamura[4], Hiroshi Miyakawa[5], Katsuhiko Hirota[6], Noriyuki Shibata[7], Hidehito Kato[1], Yutaka Arimura[1], Yoichiro Kato[7], Takehiko Uchiyama[8], Hideaki Nagamune[9], Makio Kobayashi[7], Yoichiro Miyake[6], Keiko Shiratori[3] and Junji Yagi[1]

Bacterial infection has become a focus of attention in the pathogenesis of primary biliary cirrhosis (PBC). We earlier reported that the bacterial lipoteichoic acid was detected at the sites of inflammation around damaged bile ducts in the livers of PBC, and PBC patients' sera showed high titers against streptococcal histone-like protein. Here, we investigated whether chronic bacterial exposure could trigger PBC-like epithelial cell damage in normal mouse. BALB/c mice were repeatedly inoculated with various bacteria for 8 weeks. At 1 week (Group 1) and 3, 4, or 20 months (long term; Group 2) after the final inoculation, mice were killed to obtain samples. In the livers of the *Streptococcus intermedius* (*S.i.*)-inoculated mice in Group 1, cellular infiltration was predominantly observed around the bile ducts over the hepatic parenchyma. In the *S.i.*-inoculated mice in Group 2, portal but not parenchymal inflammation was observed in the livers, and periductal cellular infiltrates were detected in the salivary glands. Both *S.i.*-inoculated Groups 1 and 2 BALB/c mice sera had antibodies against HuCCT1 biliary epithelial cells, anti-nuclear antibodies, and anti-gp210 antibodies, but not anti-mitochondrial antibodies. Immunoreactivity to histone-like DNA-binding protein of *S.i.* (*S.i.*-HLP) was detectable around the sites of chronic nonsuppurative destructive cholangitis in the portal area in the livers of both *S.i.*-inoculated Groups 1 and 2 BALB/c mice. Furthermore, anti-*S.i.*-HLP antibody bound to synthetic gp210 peptide, as well. Bacteria triggered PBC-like cholangitis, multifocal epithelial inflammation, and autoantibody production. Bacteria are likely involved in the pathogenesis of PBC and of associated multifocal epithelial inflammation.

Laboratory Investigation (2010) **90,** 577–588; doi:10.1038/labinvest.2010.40; published online 8 February 2010

KEYWORDS: bacteria; gp210; immune-mediated cholangitis; PBC; Sjögren's syndrome

The disregulation of innate and acquired immunity is known to be involved in autoimmune diseases, which are occasionally associated with multifocal organ inflammation.[1] However, the precise etiologies of these diseases have not been entirely clarified. Primary biliary cirrhosis (PBC), a slowly progressive autoimmune disease of the liver, is characterized by immune-mediated portal inflammation and destruction of the intrahepatic bile ducts and serologically by the presence of anti-mitochondrial antibodies (AMAs)[2,3] and anti-gp210.[4] As for coexisting autoimmune tissue damage characterized by multifocal epithelial inflammation, Sjögren's syndrome, hypothyroidism, renal tubular acidosis, and other conditions have been reported.[2] Although the pathogenesis of biliary epithelial cell damage in PBC is still not clearly understood, molecular mimicry has been proposed as a possible mechanism.[2,3,5–7] Reports from more than a decade ago have suggested that bacteria, particularly Gram-negative (G(−)) bacteria such as *Escherichia coli*, exhibit highly

[1]Departments of Microbiology and Immunology, Tokyo Women's Medical University, Tokyo, Japan; [2]Department of Infection Control Science and Department of Bacteriology, Faculty of Medicine, Juntendo University, Tokyo, Japan; [3]Department of Medicine and Gastroenterology, Tokyo Women's Medical University, Tokyo, Japan; [4]Department of Hepatology, Clinical Research Center, National Hospital Organization Nagasaki Medical Center, Nagasaki University Graduate School of Biomedical Sciences, Nagasaki, Japan; [5]Fourth Department of Internal Medicine, Teikyo University, Tokyo, Japan; [6]Department of Oral Microbiology, Institute of Health Biosciences, The University of Tokushima Graduate School, Tokushima, Japan; [7]Department of Pathology, Tokyo Women's Medical University, Tokyo, Japan; [8]Department of Human Science, Tokiwa University, Ibaraki, Japan and [9]Department of Biological Science and Technology, Life System, Institute of Technology and Science, The University of Tokushima Graduate School, Tokushima, Japan

Correspondence: Dr I Haruta, MD, Department of Microbiology and Immunology, Tokyo Women's Medical University, 8-1, Kawada-cho, Tokyo, Shinjuku-ku 162–8666, Japan.

E-mail: haruta@research.twmu.ac.jp

Received 22 June 2009; revised 7 December 2009; accepted 3 January 2010

conserved mitochondrial autoantigens.[6] Supporting this theory, Bogdanos *et al*[8] reported that cross-reactivity to *E. coli* mimicry was commonly seen in PBC. On the other hand, Selmi *et al*[9] reported that sera from patients with PBC exhibited positive titers for proteins from the aerobic bacteria *Novosphingobium aromaticivorans*. *N. aromaticivorans* is a G(−) bacteria whose proteins are similar to those of the human pyruvate dehydrogenase complex (PDC).[9,10] Moreover, the 16S bacterial ribosomal RNA, the sequence of which is highly homologous with that of *Staphylococcus aureus* or other Gram-positive (G(+)) bacteria,[11] has been detected in gallbladder bile and epithelioid granulomas in PBC patients.[12]

We earlier reported that the G(+) bacterial cell wall component lipoteichoic acid (LTA), an immunostimulatory molecule possessing pathogen-associated molecular patterns (PAMP),[13] was detected in the portal tract of the livers of PBC patients.[14] Recently, we reported that sera from patients with PBC exhibited higher IgM-class anti-streptococcal bacterial titers, especially to *Streptococcus intermedius* (*S.i.*). Moreover, in PBC patients' livers, immunoreactivities to anti-*S.i.* histone-like DNA-binding protein (*S.i.*-HLP) were detected in the cytoplasm of both infiltrating cells and biliary epithelial cells, around the sites of chronic nonsuppurative destructive cholangitis (CNSDC) in the portal area.[15] *S.i.* belongs to viridans group streptococci and is a commensal organism that is often found in the mouth, gastrointestinal tract, and genitourinary tract.[16] In the oral cavity, for instance, streptococci constitute approximately 60% of the initial biofilm microflora on the tooth surface.[17] Considering these observations, we speculated that some bacterial components originating from asymptomatic or less apparent chronic bacterial infection might have function(s) in the initiation and/or development of the autoimmune status in patients with PBC, eventually leading to chronic epithelial inflammation in the liver and multiple epithelial inflammation. Recently, a strain with a dominant-negative form of TGFβ receptor II,[18] IL-2 receptor $\alpha^{-/-}$ mice,[19] and $Ae2_{a,b}$-deficient mice[20] have been reported as spontaneous PBC animal models. However, as these mice are genetically engineered, they might not completely reflect the onset of human PBC. Therefore, to clarify our speculation that repeated/continuous bacterial exposures in normal mice could induce PBC-like condition, we tried to establish a mouse model to understand the pathological mechanism(s) underlying PBC.

MATERIALS AND METHODS

Bacterial Strains and Culture Conditions

The bacterial strains used were *S.i.* NCDO 2227^T, *Streptococcus sanguinis* ATCC 10556^T, *Streptococcus mitis* NCTC 12261^T, *Streptococcus salivarius* ATCC 7073^T, *Micrococcus luteus* ATCC 4698^T, *Staphylococcus epidermidis* ATCC 14990^T, and *E. coli* ATCC 25922^T All the strains were type strains. Bacteria were cultured in brain heart infusion broth (BD Biosciences) either aerobically (*M. luteus*, *S. epidermidis*, and *E. coli*) or anaerobically using the AnaeroPak system (Mitsubishi Gas Chemical) (*S.i.*, *S. sanguinis*, *S. mitis*, and *S. salivarius*). In the present series of studies, either heat-killed or live bacteria were used. Complete killing was performed by heating the bacterial suspensions at 80°C for 30 min and was confirmed by culturing for 72 h.

Mice

BALB/c mice were purchased from Crea Japan Ltd. Six-week-old female mice were used in all the experiments; all the experiments were performed in accordance with the guidelines of the ethics review committee for animal experiments at Tokyo Women's Medical University.

Treatment of Mice with Bacteria

Mice were injected with either heat-killed or live bacteria (2×10^8 CFU/mouse) in PBS; the injections were made into either the gingival mucosa (i.g.) or the intraperitoneal cavity (i.p.) twice a week for 4 weeks followed by additional injections once a week for 4 weeks. The mice were divided into two groups as summarized in Figure 1: Group 1 mice were examined 1 week after the final inoculation, and Group 2 mice were examined after a long-term experimental period (Group 2 mice inoculated with live *S.i.* were examined 3 or 4 months after the final inoculation, whereas Group 2 mice inoculated with heat-killed *S.i.* were examined 20 months after the final inoculation). Tissues and sera samples were then taken for use in the following examinations.

Histopathology

Multiple 4 μm-thick sections were deparaffinized and stained with hematoxylin and eosin. Although four stages of human PBC have been defined,[21] there is no pathological system to evaluate the disease's severity in animal PBC models. We graded the pathological scores of the damage in the portal area and hepatic parenchyma semi-quantitatively, according to the degree of the recruitment of inflammatory cells in the portal tracts accompanied by biliary epithelial cell damage: none = 0; mild = 1; moderate = 2; severe = 3; and according to the degree of cellular infiltration in hepatic parenchyma: none = 0; mild = 1; moderate = 2; severe = 3. Each group's pathological score was expressed as mean ± s.d. The scoring differences between the groups were compared using one-way ANOVA. $P < 0.05$ was considered statistically significant. Masson's trichrome staining was carried out to detect fibrosis.

Serial sections were subjected to immunohistochemical staining by incubation with mAbs against CD3 (abcam), CD45R/B220 (BD PharMingen), F4/80 antigen (BMA Biochemicals AG), TLR 2 (Santa Cruz Biotechnology, Inc.), polyclonal anti-LTA Ab (Biogenesis Inc., NH, USA), or polyclonal anti-*S.i.*-HLP[15] then stained according to a peroxidase technique using a Vectastain Elite ABC Kit (Vector Laboratories).

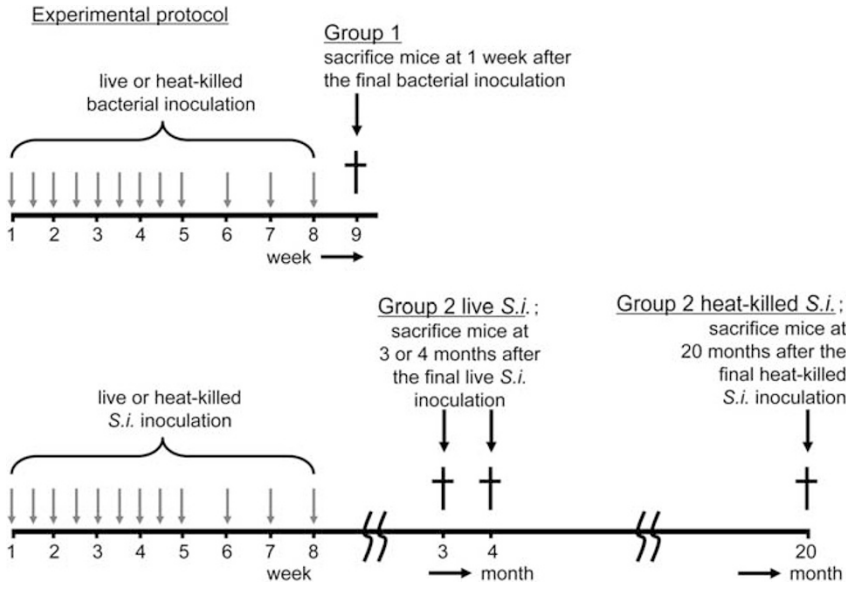

Figure 1 Experimental protocol for bacterial inoculations and schedules for killing mice to obtain samples.

Bacterial Internalization in the Biliary Epithelial Cell Line HuCCT1

Heat-killed *S.i.* was labeled with CFSE (Sigma-Aldrich). Human biliary epithelial cell line HuCCT1 cells (RIKEN Cell Bank) were cultured in RPMI 1640 supplemented with 10% FCS in glass-bottom dishes (MATSUMANI) for 24 h. The HuCCT1 cells were then incubated for an additional 16 h in the presence or absence of CFSE-labeled *S.i.* (1×10^7 CFU/ml), washed with PBS, and subjected to immunohistochemical staining. Briefly, cells were fixed with 95% ethanol, blocked with 3% nonfat milk containing 2% Triton X-100 in PBS, and stained with anti-LTA antibody (Biogenesis Inc.) followed by Cy3-conjugated anti-rabbit IgG (Jackson ImmunoResearch). Analysis was performed by using a laser scanning microscope (LSM 510; Carl Zeiss Co., Ltd.).

Phagocytotic Function of HuCCT1

HuCCT1 cells were cultured for 2 h with FITC-labeled polystyrene latex beads (Sigma) (cell:bead ratio, 25:1). After 2 h of incubation, the cells were collected after extensive washing with PBS, then analyzed using an EpicsXL flow cytometer (BECKMAN COULTER).[22]

Antibody Production in *S.i.*-Inoculated Mice

Sera were obtained from *S.i.*-inoculated BALB/c mice to study antibody production. HEp-2[23] and HuCCT1 cells were seeded onto glass-bottom dishes (MATSUNAMI), fixed with 95% ethanol, and blocked with 3% nonfat milk containing 2% Triton X-100 in PBS. The cells were then stained using a 1:100 dilution of each mouse serum in PBS followed by incubation with FITC-conjugated anti-mouse IgG (Jackson ImmunoResearch). The reactions were visualized using the LSM 510 laser scanning microscope.

Serum Reactivity to gp210

Mouse gp210 C-terminal peptide was synthesized using a peptide synthesizer (Model 432A Synergy; Applied Biosystems) and F-moc chemistry, as described earlier (24 and reference therein). The peptide was purified using reverse-phase HPLC, and a purity of $>90\%$ was attained. Using mouse p210 as an antigen, an ELISA was performed as described elsewhere.[24]

Anti-*S.i.*-HLP Reactivity to Mouse gp210

Fifty microliter of various concentration of purified gp210 oligopeptide in PBS (pH 7.6) was placed onto 96-well microplate (MaxiSorp, Nalge Nunc International K.K., Tokyo, Japan) overnight at 4°C. After washing three times with PBS, each well was blocked with 1% bovine serum albumin and then incubated with 50 μl of either 1:100 or 1:400 diluted anti-*S.i.*-HLP. After washing three times with PBS, the plates were incubated with 1:2000 diluted horseradish peroxidase-labeled goat anti-rabbit Igs (Biosource, Camarillo, CA, USA) as secondary antibody. The plates were washed three times with PBS and then incubated with peroxidase substrate, 2, 2-azino-bis-3-ethylbenthiazolin sulfonate. The reaction was stopped with sulfuric acid and cross-reactivity between gp210 and *S.i.*-HLP were measured spectrophotometrically (Vmax, Molecular Devices Inc., Tokyo, Japan) at 450 nm. Differences between groups for concentrations of gp210 and anti-*S.i.*-HLP antibodies were assessed by Mann–Whitney *U*-test. $P<0.05$ was considered to indicate a statistically significant difference.

RESULTS

Liver Pathology of Group 1 Mice in Association with Bacterial Species

In our earlier study, the serum IgM class titers specific to the *S. anginosus* group and *S.i.*-HLP were higher in patients with

PBC.[15] Therefore, in this study, we examined the induction of PBC-like CNSDC, which was triggered by chronic bacterial exposure, by using oral streptococcal species. Furthermore, the effect of the inoculation route was also compared (i.g. (see Materials and methods) *vs* i.p.). In a representative liver of Group 1 BALB/c mice inoculated with live *S.i.*, moderate pathological findings were observed in the portal area, as revealed by enlarged portal tracts accompanied by moderate inflammatory cellular infiltrate of lymphocytes, plasma cells, granulocytes, and biliary epithelial cell damage with a focal disruption of the basement membrane; on the other hand, inflammation in the hepatic parenchyma was mild. A similar degree of portal inflammation induced both i.g. and i.p. after *S.i.* inoculation. The inoculation route did not significantly affect the pathological scores of portal inflammation (Figures 2a, b, and 3). In heat-killed *S.i.*-inoculated BALB/c mice, moderate to severe portal inflammation was observed, whereas inflammation in hepatic parenchyma was mild (Figure 2c and d). The inoculation route did not affect the pathological scores of portal inflammation (Figure 3).

In live *S. sanguinis* i.g.-inoculated BALB/c mice, moderate to severe changes in both portal inflammation and biliary epithelial cell damage were also observed with moderate but less score of inflammation in hepatic parenchyma (Figure 2e). In live *S. mitis* i.g.-inoculated BALB/c mice, moderate inflammation was observed in both the portal area and hepatic parenchyma (Figure 2f). Live *M. luteus* i.g. innoculation and heat-killed *E. coli* i.p. inoculation induced mild inflammation around the portal tracts and hepatic parenchyma (Figure 2g and h). In PBS-inoculated BALB/c mice, both inflammatory cellular infiltrates and biliary epithelial cell damage around the portal tracts and hepatic parenchyma were the mildest among the groups (Figure 2i). The pathological scores are summarized in Figure 3.

Among the live *S. salivarius*-inoculated BALB/c mice, four of the five mice died before the completion of the inoculation

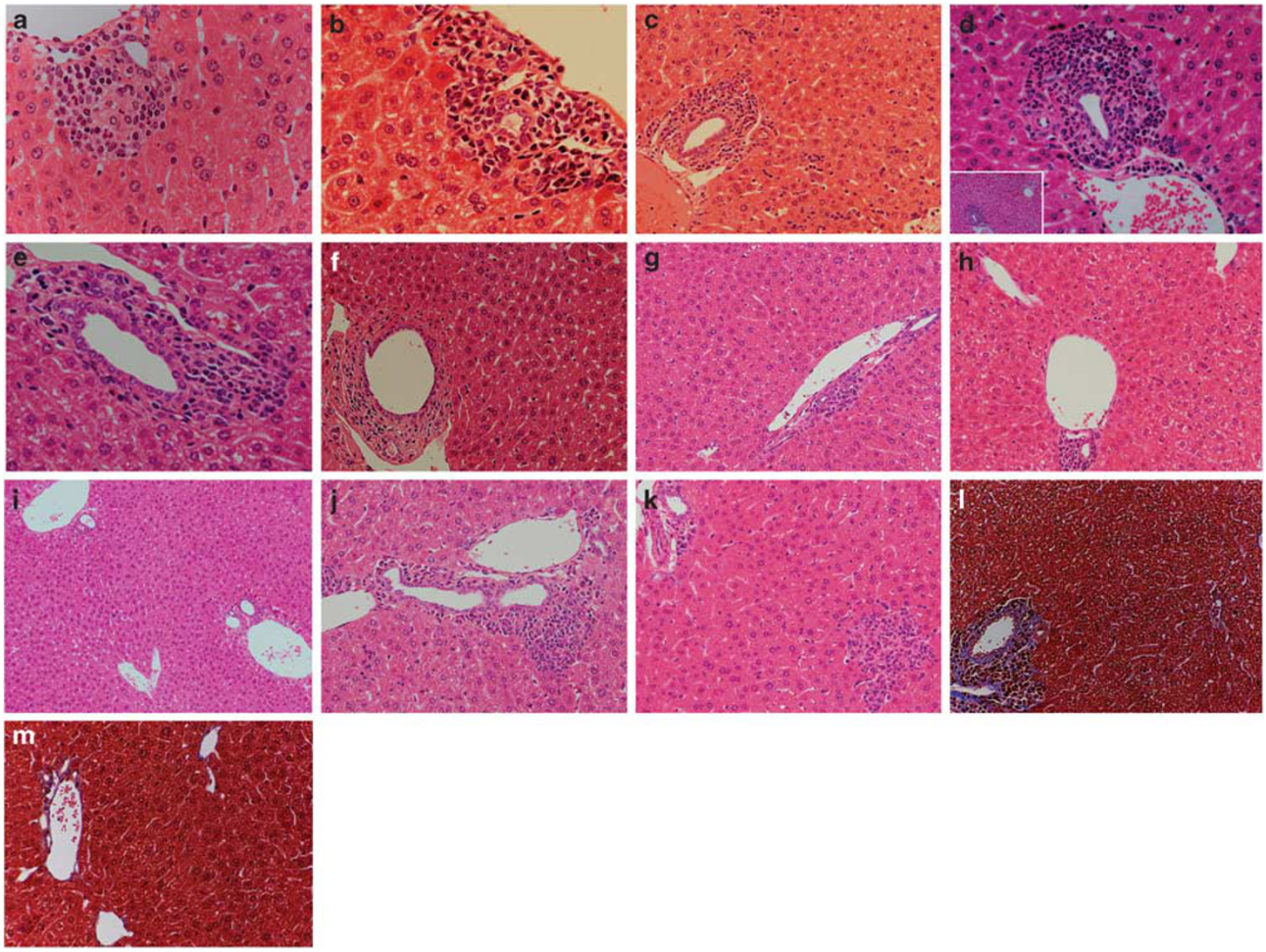

Figure 2 Representative pathological findings for Group 1 mouse livers. BALB/c mouse livers inoculated with live *S.i.* i.g. (**a**), live *S.i.* i.p. (**b**), heat-killed *S.i.* i.g.(**c**), heat-killed *S.i.* i.p (left lower corner shows a lower magnification) (**d**), live *S. sanguinis* i.g. (**e**), live *S. mitis* i.g. (**f**), live *M. luteus* i.g. (**g**), heat-killed *E. coli* i.p. (**h**), PBS, without bacterial inoculation (**i**), live *S. salivarius* i.g. (**j**), or live *S. epidermidis* i.g. (**k**) (hematoxylin and eosin). Representative Masson's Trichrome staining profiles of the liver in heat-killed *S.i.* i.p.-inoculated (**l**), and PBS-injected (**m**) Group 1 BALB/c mice (hematoxylin and eosin). ($n = 4$–9 for each group).

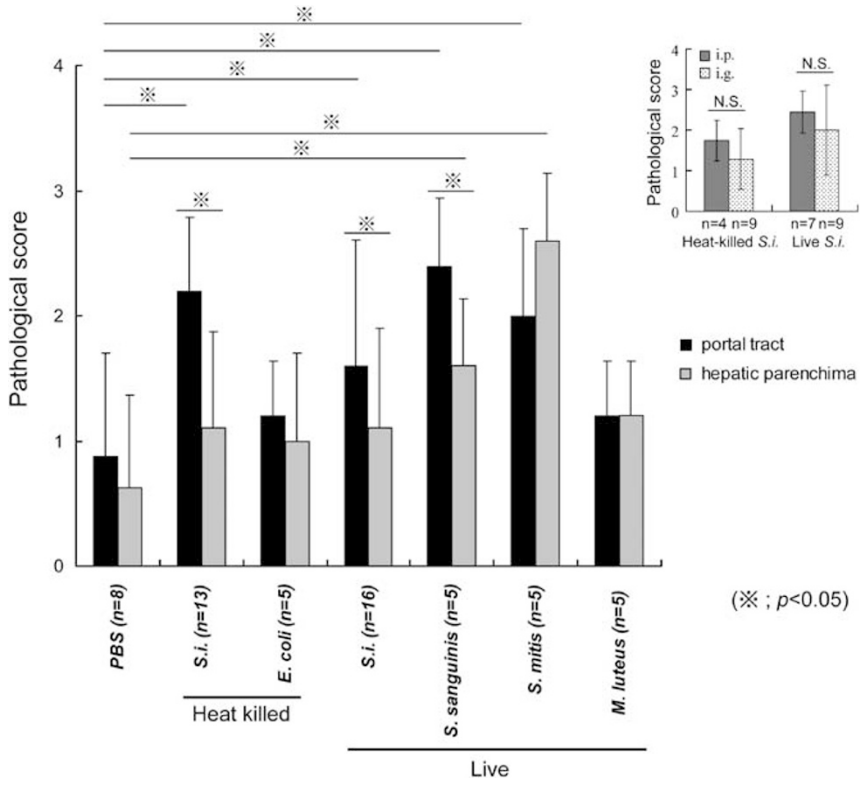

Figure 3 Pathological scores for the livers of Group 1 BALB/c mice. The bars indicate the mean pathological score of each group, and the error bar indicates s.d. Right upper graph represents comparisons between the bacterial-inoculation route, that is i.p. *vs* i.g., in both heat-killed and live *S.i.*-inoculated groups. Heat-killed *S.i.*-inoculated mice ($n=13$) consisted of i.p.-inoculated ($n=4$) and i.g.-inoculated mice ($n=9$). Live *S.i.*-inoculated mice ($n=16$) included i.p.-inoculated ($n=7$) and i.g.-inoculated mice ($n=9$). The bars indicate mean the pathological score of each group, and the error bar indicates s.d. ($^*P<0.05$).

schedule. In the one remaining mouse, the portal area was severely inflamed (Figure 2j). Among the live *S. epidermidis*-inoculated BALB/c mice, three of the five mice died before the completion of the inoculation schedule. In the two remaining mice, the portal inflammation in the liver was mild, although granulomatous sinusoidal inflammation was observed (Figure 2k).

Masson's trichrome-positive fibrous stroma was markedly detected at the site of portal inflammation in both the heat killed (Figure 2l) and the live (data not shown) *S.i.*-inoculated BALB/c mice livers. On the other hand, fibrous stroma was less detectable in the PBS-inoculated BALB/c mice (Figure 2m). Thus, in the Group 1 mice, *S.i., S. sanguinis*, and *S. salivarius* inoculation induced distinct portal inflammation. In light of these bacterial effects on the liver, we selected live or heat-killed *S.i.* for use in further studies.

Pathology of Group 2 BALB/c Mice without Further Bacterial Inoculations

Considering that the peak incidence of PBC occurs in the fifth decade of life and that it is uncommon in persons under 25 years of age,[2] we investigated the long-term pathological alterations in additional *S.i.*-inoculation-free BALB/c mice after the completion of *S.i.* inoculation, that is Group 2 mice. Three to 4 months after the final live *S.i.* inoculation, moderate portal inflammation was still observed, whereas mild or no inflammation was found in the hepatic parenchyma. There were no significant differences in the severity of portal inflammation between 3 and 4 months after the final live *S.i.* inoculation (Figure 4a, A and B). Even 20 months after the final heat-killed *S.i.* inoculation, the portal tracts were still enlarged, and marked inflammatory cellular infiltrates and biliary epithelial cell damage, such as focal disruptions of the basement membrane in the portal area, were observed, whereas mild to no inflammation was found in the hepatic parenchyma (Figure 4a, C and D). In the mice killed 20 months after the final PBS inoculation, mild to no inflammation was present around the bile ducts or in the hepatic parenchyma (Figure 4a, E). Masson's trichrome-positive fibrous stroma was markedly detected at the site of portal inflammation in the liver (Figure 4a, F and G). Thus, the PBC-like pathological alterations in the livers of mice inoculated with *S.i.* persisted for a long time without exogenous bacterial stimuli and became more restricted in the portal area, followed by fibrosis. Pathological scores are summarized in Figure 4a, H.

Other tissue damages that are occasionally associated with PBC were examined in Group 2 *S.i.*-inoculated BALB/c mice. The salivary glands of live *S.i.*-inoculated mice showed mild periductular lymphocytic infiltration in two of the six mice

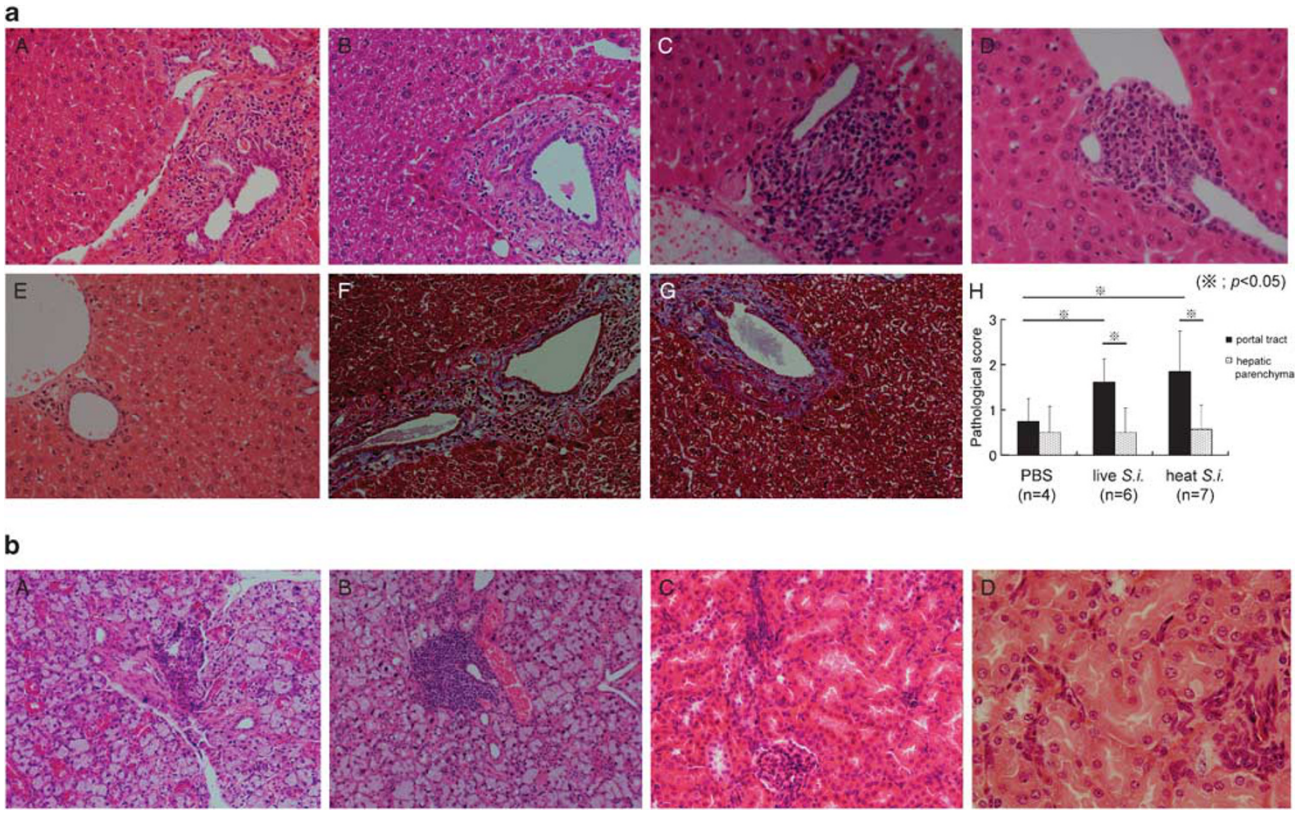

Figure 4 Representative pathological findings of Group 2 BALB/c mice. (**a**) Liver from a mouse inoculated with live *S.i.* 3 months (A) or 4 months (B) after the final inoculation and in a mouse inoculated with heat-killed *S.i.* (C, D) or PBS (E) 20 months after the final inoculation (hematoxylin and eosin). Three months (F) and 20 months (G) after the final live *S.i.* inoculation (Masson's trichrome). (H) Pathological scores for the livers of Group 2 *S.i.*-inoculated BALB/c mice. The bars indicate the mean pathological score of each group, and the error bar indicates s.d. (*$P<0.05$). (**b**) Salivary glands and kidneys from Group 2 BALB/c mice. Salivary glands from a mouse inoculated with live *S.i.* (A) and from a mouse inoculated with heat-killed *S.i.* (B). Kidneys from a mouse inoculated with live *S.i.* (C) and from a mouse inoculated with heat-killed *S.i.* (D) (hematoxylin and eosin).

(33%) (Figure 4b, A). Heat-killed *S.i.*-inoculated mice exhibited moderate to marked lymphocytic infiltrations around the ducts in five of the seven (71%) mice (Figure 4b, B). The kidneys showed mild to moderate inflammatory cellular infiltrates around the basal lesions of the renal tubules in five of the six (83%) live *S.i.*-inoculated mice and four of the seven (57%) heat-killed *S.i.*-inoculated mice (Figure 4b, C and D, respectively). The pancreas had almost no inflammatory cellular infiltrates in the live *S.i.*-inoculated mice, and mild inflammatory cellular infiltrates around the pancreatic duct in only one of the seven (14%) heat-killed *S.i.*-inoculated mice (data not shown). Thus, some, but not all, of the repeated *S.i.*-inoculated mice revealed systemic epithelial inflammation similar to that seen in PBC.[3]

Cellular Infiltrates in the Livers of Group 2 *S.i.*-Inoculated BALB/c Mice

To clarify the cell subsets infiltrating in the livers, we next performed immunohistochemical staining. In the *S.i.*-inoculated Group 2 mice, CD3-positive cells were predominantly observed in the cellular infiltrates around the bile ducts (Figure 5a, A and B), whereas relatively few B220-immunoreactive or F4/80 pan-macrophage antigen-immunoreactive cells were observed (Figure 5a, C and D). TLR2 immunoreactivities were also detectable in the cytoplasm of some, but not all, infiltrating cells (Figure 5a, E). Thus, *S.i.* inoculation triggers innate immunity and inflammation, as suggested by the TLR2 expression pattern, which might be involved in the upregulation of CD3-positive cell-mediated immune responses. In Group 2, heat-killed *S.i.*-inoculated mouse salivary glands, CD3-positive cells (Figure 5b, A), B220-immunoreactive cells (Figure 5b, B), and TLR2 immunoreactive cells were detected in the cytoplasm of some, but not all, of the infiltrating cells around the ducts (Figure 5b, C).

Detection of Bacterial Component in the Liver of *S.i.*-Inoculated Mice

The involvement of bacterial exposures in the pathogenesis of PBC was examined more directly by detecting the presence of bacterial component in the liver of live *S.i.* inoculated both Groups 1 and 2 BALB/c mice. LTA immunoreactivity was detectable in not all, but some of the cytoplasm of polymorphic inflammatory cells around biliary epithelial cells and connective tissues around bile ducts (Figure 5c, A and B, respectively).

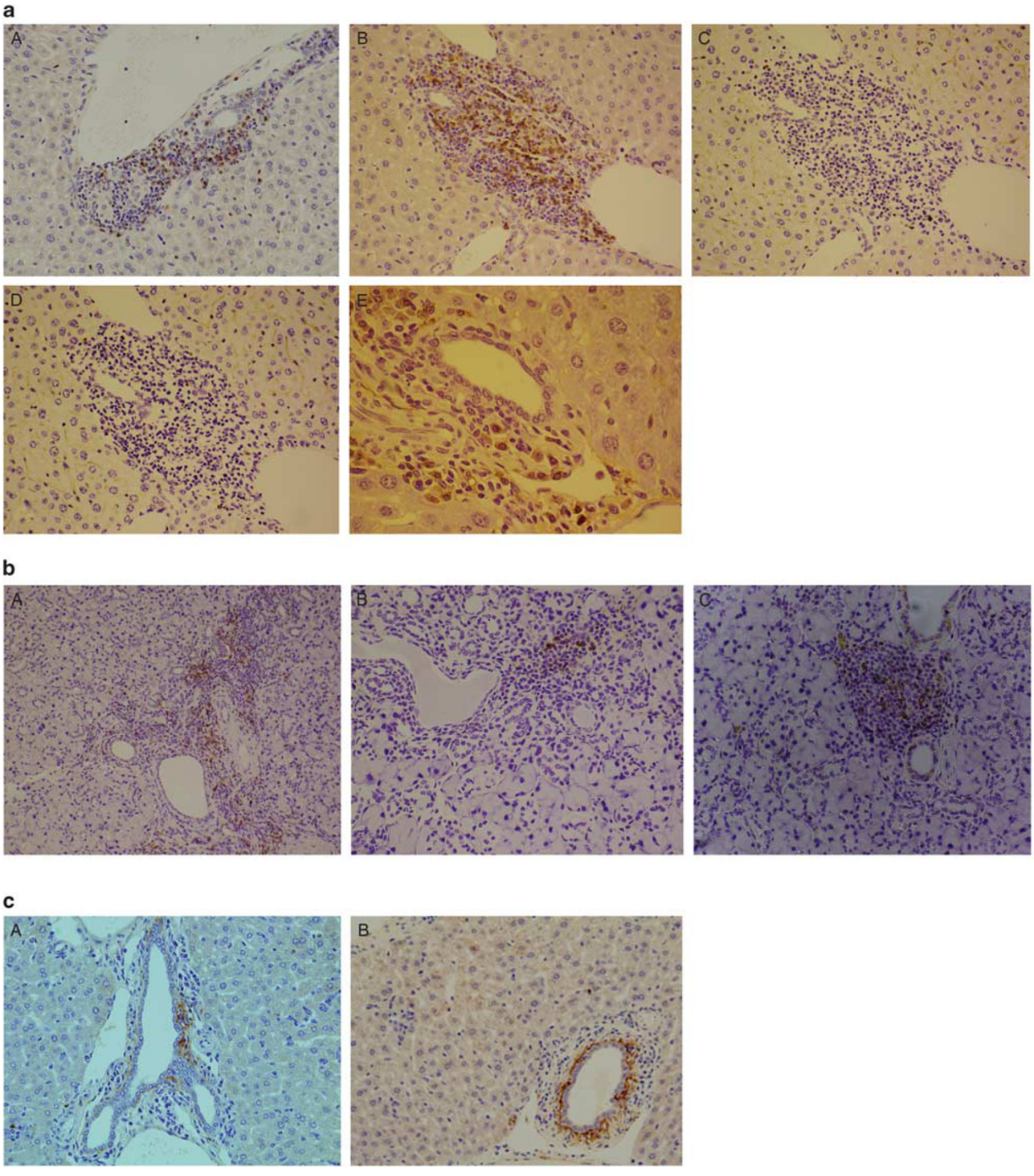

Figure 5 Immunostaining of various molecules in *S.i.*-inoculated Group 2 BALB/c mice. (**a**) Immunoreactivities to CD3 (A, B), B220 (C), F4/80 antigen (D), and TRL2 (*e*) in the liver. (**b**) Immunoreactivities to CD3 (A), B220 (B) and TRL2 (C) in the salivary glands. (**c**) Immunoreactivities to LTA in Group 1 (A) and Group 2 (B) *S.i.*-inoculated BALB/c mice.

Immunoreactivity to *S.i.*-HLP

Immmunoreactivities to *S.i.*-HLP were studied using *S.i.*-inoculated BALB/c mice. In the livers of Group 1 mice, immunoreactivities to anti-*S.i.*-HLP were detected at the cytoplasm of some inflammatory cells around bile ducts (Figure 6a). In the livers of Group 2 mice, both 3 to 4 and 20 months after the final *S.i.* inoculation, immunoreactivities to anti-*S.i.*-HLP were detected at the cytoplasm of inflammatory cells around the bile ducts (Figure 6b and c, respectively), whereas numbers of *S.i.*-HLP immunoreactive

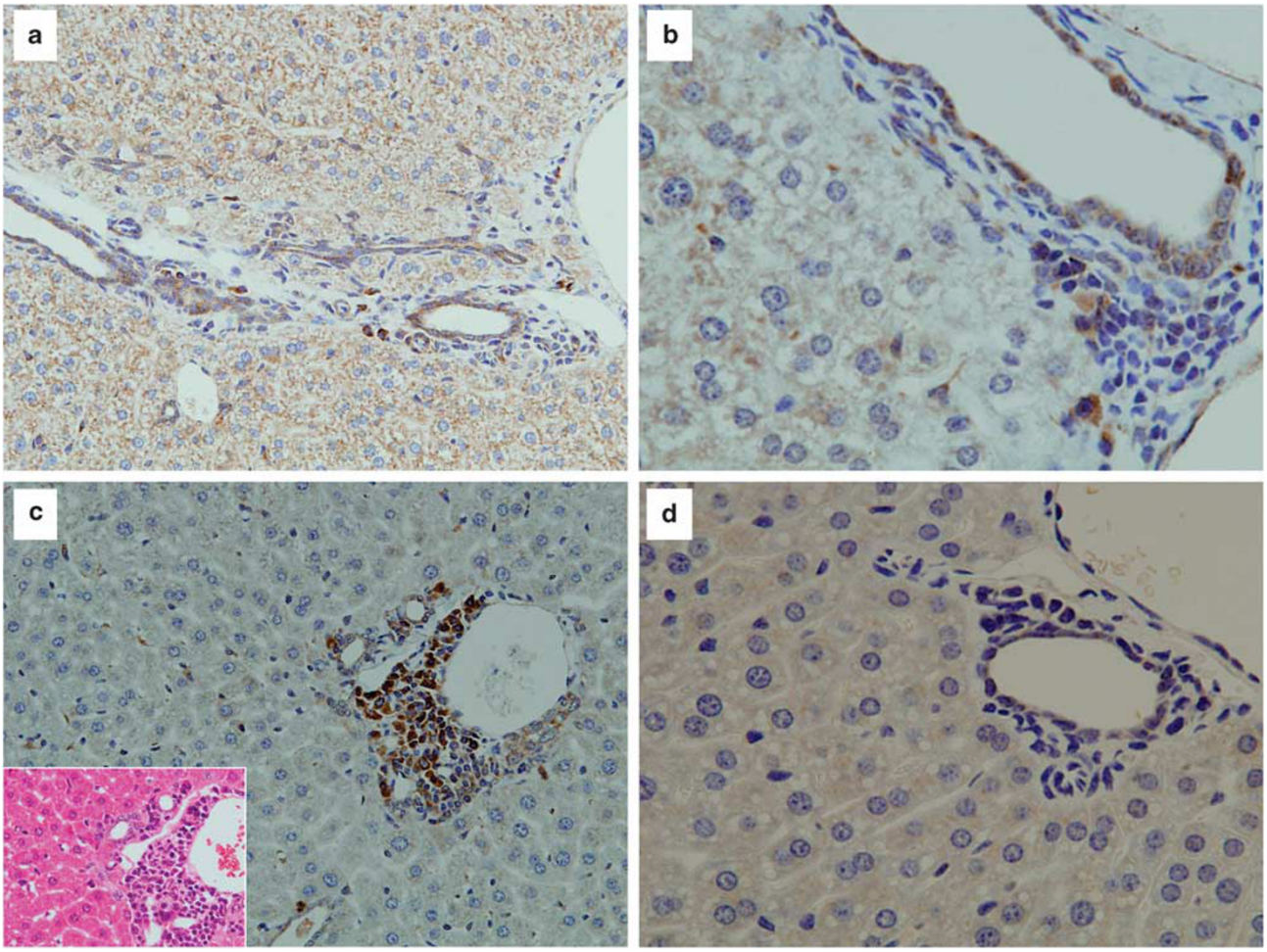

Figure 6 Immumoreactivities to *S.i.*-HLP. Group 1 *S.i.*-inoculated BALB/c mice liver (**a**), Group 2 *S.i.*-inoculated BALB/c mice liver, which was 3 months after the final *S.i.* inoculation (**b**), Group 2 *S.i.*-inoculated BALB/c mice liver, which was 20 months after the final *S.i.* inoculation (**c**) (left lower corner of (**c**) shows hematoxylin and eosin), and Group 2 PBS-inoculated BALB/c mice liver (**d**).

inflammatory cells were much higher in 20 months mice livers than 3–4 months mice livers. Interestingly, immunoreactivities to anti-*S.i.*-HLP were also detected in some of the biliary epithelial cells in Group 2 mice livers (Figure 6b). On the other hand, immunoreactivity to anti-*S.i.*-HLP was not detected in the livers of PBS-inoculated Group 2 mice (Figure 6d).

Internalization of *S.i.* by Epithelial Cell Line

Epithelial cells may have direct functions in both the capture of *S.i.* antigens and the induction of tissue damage. To examine this possibility, an imaging analysis was performed after the incubation of the HuCCT1 biliary epithelial cell line with CSFE-labeled *S.i.* Confocal microscopic images showed both the extracellular and the intracellular localization of *S.i.* (Figure 7a, A), which was also immunoreactive to anti-LTA Ab (Figure 7a, B). The merged images indicated that this cell line internalized *S.i.* (Figure 7a, C). In addition, HuCCT1 cells showed a phagocytotic function, earlier suggested elsewhere,[25] as revealed using FITC-labeled polystyrene latex beads (Figure 7b).

Production of Autoantibodies

Finally, we examined whether PBC-like autoantibodies were produced in our model or not. The *S.i.*-inoculated BALB/c mice developed antibodies that reacted to both the cytoplasm and nuclei of HuCCT1 epithelial cells (Figure 7c, A and B, for Group 1 live and Group 2 heat-killed *S.i.*-inoculated mice, respectively). On the other hand, PBS-inoculated BALB/c mice did not develop antibody to HuCCT1 (Figure 7c, C). However, AMAs against the E2 subunit of PDC-E2, the E2-subunit of the branched-chain 2-oxoacid dehydrogenase complex (BCOADC-E2), and the 2-oxoglutarate dehydrogenase complex (OGDC-E2) were all negative by western blot analysis (data not shown), in both Groups 1 and 2 mice sera. Group 2 *S.i*-inoculated BALB/c mice also produced antinuclear antibodies (ANAs), as shown by staining using HEp2 cells (Figure 7d, A), whereas, in the Group 1 *S.i.*-inoculated BALB/c mice, the titers for ANAs seemed to

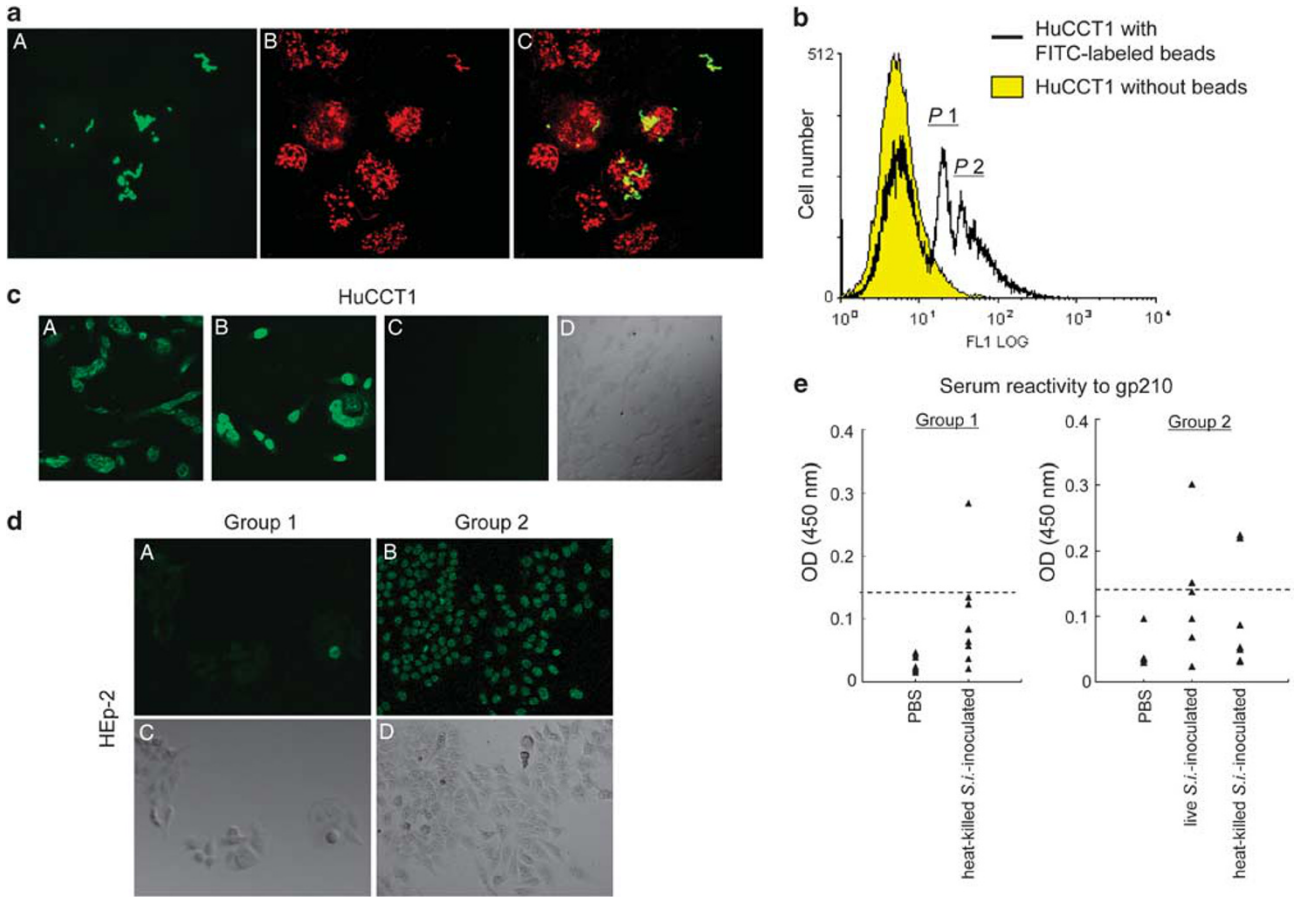

Figure 7 Uptake of *S.i.* by biliary epithelial cells and induction of autoantibodies in Groups 1 and 2 mice sera. (**a**) Internalization of *S.i.* by the epithelial cell line HuCCT1. CFSE-labeled heat-killed *S.i.* were co-cultured with HuCCT1 cells for 16 h, then washed with PBS, fixed, and subjected to immunohistochemical staining. (A) Green fluorescence images indicating CFSE-labeled *S.i.* (B) LTA immunoreactivities represented by Cy3-red fluorescence images. (C) Merged images of both CSFE-labeled *S.i.* and LTA immunoreactivities. (**b**) HuCCT1 cells showed the phagocytosis of FITC-labeled polystyrene latex beads. HuCCT1 cells were cultured for 2 h with appropriate numbers of FITC-labeled polystyrene latex beads. The cells were collected followed by extensive washing with PBS, then analyzed by fluorocytometry. Peak (*P*)1–*P*2 corresponded to the number of phagocytized beads. (**c**) Serum antibodies to HuCCT1 and ANA in Groups 1 and 2 *S.i.*-inoculated BALB/c mice. Immunoreactivities to HuCCT1 cells, using sera from Group 1 live *S.i.*-inoculated mice (A), Group 2 heat-killed *S.i.*-inoculated (B) and Group 2 PBS-inoculated BALB/c mice (C, D) (DIC image of (C)). (**d**) Detection of ANA using HEp-2 cells in sera from Group 1 *S.i.*-inoculated mice (A) and Group 2 heat-killed *S.i.*-inoculated mice (B). (C, D): DIC images of (A, B), respectively. (**e**) Anti-gp210 reactivities of BALB/c mice sera, as measured using an ELISA. Sera were obtained from Group 1 PBS-injected ($n=10$), heat-killed *S.i.*-inoculated ($n=9$), and Group 2 PBS-injected ($n=4$), live *S.i.*-inoculated ($n=6$) and heat-killed *S.i.*-inoculated ($n=7$) mice. The dotted line shows the mean OD value of the Group 2 PBS-injected mice + 3s.d.

be much lower than those in Group 2 (Figure 7d, B). As anti-gp210 antibodies have been detected in patients with PBC,[4,24] anti-gp210 reactivity was measured using an ELISA. When the OD value exceeded the mean OD value of the Group 2 PBS-injected mice + 3 s.d., we defined the sample as being positive for anti-gp210 antibody induction. On the basis of this definition, one of the nine (11.1%) Group 1 heat-killed *S.i.*-inoculated mice, two of the six (33.3%) Group 2 live *S.i.*-inoculated mice, and two of the seven (28.5%) Group 2 heat-killed *S.i.*-inoculated BALB/c mice were anti-gp210 positive (Figure 7e).

Anti-*S.i.*-HLP Reactivity to Mouse gp210

Fixed concentration of polyclonal anti-*S.i.*-HLP (1/400 dilution) was reacted with gp210 peptide, dose-dependent manner (200 ng/well:500 ng/well = 0.209 ± 0.020:0.593 ± 0.132, $P<0.05$) by ELISA (Figure 8a). In addition, when coated, gp210 peptide was fixed at 200 ng/well, OD value was changed depending on the concentration of anti-*S.i.*-HLP Ab (1/400 dilution:1/100 dilution = 0.209 ± 0.020:0.426 ± 0.080, $P<0.05$) (Figure 8b). These results suggested the molecular mimicry of gp210 peptide to *S.i.*-HLP.

DISCUSSION

In Group 1 BALB/c mice, examined in the early period after the final inoculation, *S.i.* and *S. sanguinis* showed distinct portal inflammation (Figure 2). *S.i.*, *S. sanguinis*, and *S. salivarius* all belong to the viridans group streptococci.[26] These microorganisms grow preferentially in the oral cavity, attaching to a surface, forming matrix-enclosed biofilms, and

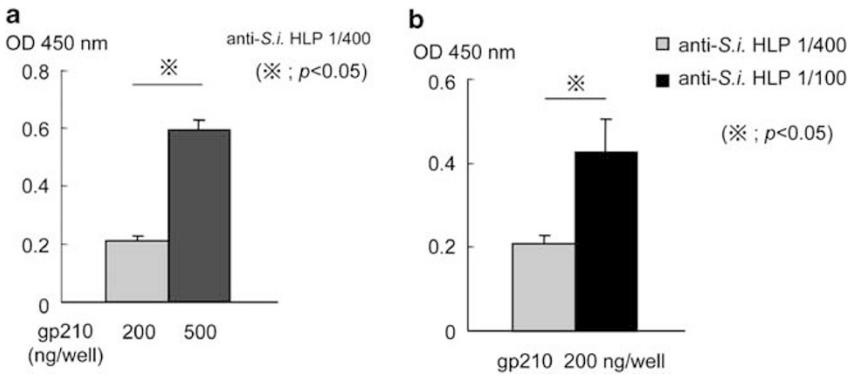

Figure 8 Anti-*S.i.*-HLP reactivity to mouse gp210. Either 200 or 500 ng/well of synthetic gp210 peptide-coated plates were used for ELISA. Reactivities to 1/400 diluted polyclonal anti-*S.i.*-HLP Ab were measured by OD 450 nm (**a**). Reactivity to 200 ng/well of gp210 peptide was studied using either 1/400 or 1/100 diluted polyclonal anti-*S.i.*-HLP Ab (**b**).

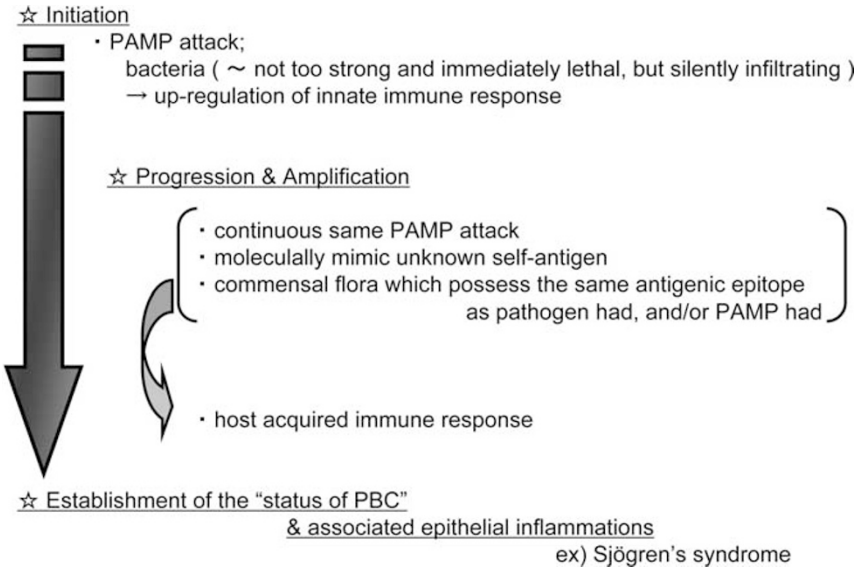

Figure 9 Hypothetical pathogenesis of PBC. The slowly progressing steps by the persistence of the PAMP attack or a molecularly mimic antigen or stimuli from commensal flora would complete to generate PBC-like nonsuppurative destructive cholangitis.

thereby exhibiting increased resistance to antimicrobials and to host immune defense mechanisms.[27] It is possible that, except for cases, which were severe lethal infection, most of these bacteria would remain in place, and provide a chronic and silent pathogen supply with which the status of PBC could mature. Supporting this notion, viridans group streptococci were actually detected from PBC patients' oral mucosa (unpublished observation). In Group 1 *S.i.*-inoculated BALB/c mice, both live and heat-killed *S.i.* effectively induced portal inflammation pathologically. Not only live bacteria, but some bacterial components might be capable of inducing portal inflammation.

We investigated pathological alterations in long-term additional *S.i.*-inoculation-free BALB/c mice, after completing repeated *S.i.* inoculation, that is Group 2 mice. In both Group 2 live and heat-killed *S.i.*-inoculated BALB/c mice, the predominance of portal inflammation over inflammation of the hepatic parenchyma became much clearer (Figure 4), when compared with Group 1 mice (Figure 2). Group 2 mice also exhibited duct-centric inflammation in the salivary gland and moderate to marked inflammation around the basal regions of renal tubules. These pathological alterations closely resembled the pathological feature of occasionally associated tissue damage in PBC.[3] Thus, the human PBC-like pathological changes persisted and were generated for a long time in the absence of exogenous bacterial stimuli.

From the results of this study, we imagine the following scenario. As HuCCT1 biliary epithelial cells internalized *S.i.* and showed a phagocytotic function (Figure 7), the biliary epithelial cells and other associated tissues may present and/or provide digested bacterial antigens to immune cells, triggering innate immunity and CD3-positive cell infiltrates (Figure 5). Perhaps, then the extent of the inflammation might have been maintained by stimuli from commensal

bacteria, such as oral bacteria or gut flora, even after the completion of the *S.i.* inoculations. This is suggested by the presence of LTA, *S.i.*-HLP, and the upregulation of TLR2 in the portal area in Group 2 mice (Figures 5 and 6), and might ultimately result in the establishment of systemic PBC-like pathological changes. *S.i.*-HLP was found to bind host cells and induce cytokine production.[28] It was reported that stimulation with recombinant *S.i.*-HLP (r*S.i.*-HLP) induced the secretion of IL-8, IL-1β, and tumor necrosis factor-α in human monocytic cell line THP-1. The stimulatory effect of r*S.i.*-HLP was cooperative by costimulation with LTA.[29] Upregulation of serum pro-inflammatory cytokines, complements, and soluble interleukin 2 receptor in PBC was reported.[30] Therefore, kinetic studies including cytokine and complement changes in our mice model are needed.

Alternatively, or additionally, an autoantigen might exist or might be generated by modification through inflammation in the epithelial cells of the bile duct as well as in other associated tissues, which might mimic the *S.i.* antigen, thereby becoming a target of *S.i.*-induced immune responses and resulting in damage to specific tissues. To clarify this possibility, the identification of an autoantigen is obviously necessary and further investigation of this topic is now underway. One possible autoantigen might be gp210, as suggested by the production of anti-gp210 antibodies in *S.i.*-inoculated mice sera and the cross-reactivities between gp210 peptide and anti-*S.i.*-HLP (Figures 7 and 8). It remains to be elucidated whether or not the CD3-positive cell infiltrates (Figure 5) represent autoreactive T cells to a molecular mimic an autoantigen.

We also detected autoantibody production. Both Groups 1 and 2 *S.i.*-inoculated BALB/c mice generated antibodies reactive with HuCCT1 biliary epithelial cells. Furthermore, Group 2 *S.i.*-inoculated BALB/c mice generated ANA (Figure 7). In addition, 11.1% of Group 1 heat-killed *S.i.*-inoculated mice, 33.3% of Group 2 live *S.i.*-inoculated mice, and 28.5% of Group 2 heat-killed *S.i.*-inoculated BALB/c mice were positive for anti-gp210 (Figure 7e). In earlier studies, sera from a subgroup of human PBC patients were reportedly positive for ANAs,[4] and anti-gp210 has been detected in about 32% of PBC patients.[24] From this viewpoint, our repeatedly *S.i.*-inoculated mouse model might also be useful as a natural PBC-like autoimmune cholangitis model. However, our observations indicated that AMAs against the PDC-E2, BCOADC-E2, and OGDC-E2, which are usually positive in the sera of patients with PBC,[1] were all negative by western blot analysis (data not shown). Sera from a subgroup of patients, including some AMA-negative patients, are positive for ANAs.[31] These ANAs include two components of the nuclear pore complex specifically associated with a perinuclear pattern, that is gp210 and p62, Sp100, and promyelocytic leukemia proteins.[4] Taken together, our observation might indicate one of the possible pathogeneses of PBC, that is the interaction between bacterial HLP, such as *S.i.*-HLP and/or eukaryotic histone with gp210 could have some pathological function(s) on the initiation or progression of PBC. Thus, our model might reflect the pathogenesis of AMA-negative PBC.

In conclusion, we propose the hypothetical pathogenesis of PBC shown in Figure 9. In the initiation phase, a not too strong, but silently, infiltrating PAMP or antigen(s), such as bacterial HLP,[32] would trigger and upregulate the innate immune system. Second, the progression phase would feature the persistence of this PAMP attack or a molecularly mimic antigen, for example unknown self-antigen, bacterial HLP and/or gp210, exposure, or stimuli from commensal flora possessing the same antigenic epitope that the pathogen and/or PAMP had, making the host immune response for the target antigen upregulated. These slowly progressing steps would complete to generate the status of PBC. Investigation of the pathological mechanism in detail in this model would give us new hints toward a therapeutic approach for autoimmune epithelial inflammation, such as PBC.

ACKNOWLEDGEMENTS

We thank Hideyuki Takeiri, Noriko Sakayori, Mizuho Karita, Naoko Kodama, and Yasuhide Shigematsu for their skillful technical assistance, Tohru Miyoshi-Akiyama and Hidehiro Ueshiba for their help in the series of bacterial inoculations of mice, and Masamichi Yoshikawa for the intensive animal care. This work was supported in part by grants from the Ministry of Education, Culture, Sports, Science, and Technology of Japan.

DISCLOSURE/CONFLICT OF INTEREST

The authors declare no conflict of interest.

1. Krieg AM, Vollmer J. Toll-like receptors 7, 8, and 9: linking innate immunity to autoimmunity. Immunol Rev 2007;220:251–269.
2. Kaplan MM, Gershwin ME. Primary biliary cirrhosis. New Engl J Med 2005;353:1261–1273.
3. Portmann BC, Nakanuma Y. Disease of the bile ducts. In: MacSween RNM, Burt AD, Portmann BC, Ishak KG, Scheuer PJ, Anthony PP, (eds). Pathology of the Liver. Churchill Livingstone: London, UK, 2002, pp 435–506.
4. Invernizzi P, Selmi C, Ranftler C, *et al.* Antinuclear antibodies in primary biliary cirrhosis. Semin Liver Dis 2005;25:298–310.
5. Nishio A, Keeffe EB, Gershwin ME. Immunopathogenesis of primary biliary cirrhosis. Semin Liver Dis 2002;22:291–302.
6. Fussey SP, Ali ST, Guest JR, *et al.* Reactivity of primary biliary cirrhosis with *Escherichia coli* dihydrolipoamide acetyltransferase (E2p): characterization of the main immunogenic region. Proc Natl Acad Sci USA 1990;87:3987–3991.
7. Selmi C, Gershwin ME. Bacteria and human autoimmunity: the case of primary biliary cirrhosis. Curr Opin Rheumatol 2004;16:406–410.
8. Bogdanos DP, Baum H, Butler P, *et al.* Association between the primary biliary cirrhosis specific anti-sp100 antibodies and recurrent urinary tract infection. Dig Liver Dis 2003;35:801–805.
9. Selmi C, Balkwill DL, Invernizzi P, *et al.* Patients with primary biliary cirrhosis react against a ubiquitous xenobiotic-metabolizing bacterium. Hepatology 2003;38:1250–1257.
10. Kaplan MM. Novosphingobium aromaticivorans: a potential initiator of primary biliary cirrhosis. Am J Gastroenterol 2004;99:2147–2149.
11. Harada K, Tsuneyama K, Sudo Y, *et al.* Molecular identification of bacterial 16S ribosomal RNA gene in liver tissue of primary biliary cirrhosis: is propionibacterium acnes involved in granuloma formation? Hepatology 2001;33:530–536.
12. Hiramatsu K, Harada K, Tsuneyama K, *et al.* Amplification and sequence analysis of partial bacterial 16S ribosomal RNA gene in gallbladder bile from patients with primary biliary cirrhosis. J Hepatol 2000;33:9–18.

13. Henneke P, Morath S, Uematsu S, *et al.* Role of lipoteichoic acid in the phagocyte response to group B streptococcus. J Immunol 2005;174:6449–6455.
14. Haruta I, Hashimoto E, Kato Y, *et al.* Lipoteichoic acid may affect the pathogenesis of bile duct damage in primary biliary cirrhosis. Autoimmunity 2006;39:129–135.
15. Haruta I, Kikuchi K, Hashimoto E, *et al.* A possible role of histone-like DNA-binding protein of Streptococcus intermedius in the pathogenesis of bile duct damage in primary biliary cirrhosis. Clin Immunol 2008;127:245–251.
16. Whiley RA, Beighton D, Winstanley TG, *et al. Streptococcus intermedius*, *Streptococcus constellatus*, and *Streptococcus anginosus* (the Streptococcus milleri group): association with different body sites and clinical infections. J Clin Microbiol 1992;30:243–244.
17. Petersen FC, Pecharki D, Scheie AA. Biofilm mode of growth of Streptococcus intermedius favored by a competence-stimulating signal peptide. J Bacteriol 2004;186:6327–6331.
18. Oertelt S, Lian ZX, Cheng CM, *et al.* Anti-mitochondrial antibodies and primary biliary cirrhosis in TGF-β receptor II dominant-negative mice. J Immunol 2006;177:1655–1660.
19. Wakabayashi K, Lian Z-X, Moritoki Y, *et al.* IL-2 receptor $\alpha^{-/-}$ mice and the development of primary biliary cirrhosis. Hepatology 2006;44:1240–1249.
20. Salas JT, Banales JM, Sarvide S, *et al.* $Ae2_{a,b}$-deficient antimitochondrial antibodies and other features resembling primary biliary cirrhosis. Gastroenterology 2008;134:1482–1493.
21. Scheuer PJ. Primary biliary cirrhosis. Proc R Soc Med 1967;60: 1257–1260.
22. Haruta I, Kato Y, Hashimoto E, *et al.* Association of AIM, a novel apoptosis inhibitory factor, with hepatitis via supporting macrophage survival and enhancing phagocytotic function of macrophages. J Biol Chem 2001;276:22910–22914.
23. Bogdanos DP, Invernizzi P, Mackay IR, *et al.* Autoimmune liver serology: current diagnostic and clinical challenges. World J Gastroenterol 2008;14:3374–3387.
24. Nakamura M, Shimizu-Yoshida Y, Takii Y, *et al.* Antibody titer to gp210-C terminal peptide as a clinical parameter for monitoring primary biliary cirrhosis. J Hepatol 2005;42:386–392.
25. Allina J, Hu B, Sullivan DM, *et al.* T cell targeting and phagocytosis of apoptotic biliary epithelial cells in primary biliary cirrhosis. J Autoimmun 2006;27:232–241.
26. Murrray PR, Rosenthal KS, Kobayashi GS, *et al.* Streptococcus. Schmitt W, Grigg LL (eds). Medical Microbiology. Mosby, Inc., A Harcourt Health Science Company: London, UK, 2002, pp 217–235.
27. Petersen FC, Pecharki D, Scheie AA. Biofilm mode of growth of Streptococcus intermedius favored by a competence-stimulating signal peptide. J Bacteriol 2004;186:6327–6331.
28. Liu D, Yumoto H, Murakami K, *et al.* The seesntiality and involvement of Streptococcus intermedius histone-like DNA-bundung protein in bacterial viability and normal growth. Mol Microbiol 2008;68: 1268–1282.
29. Liu D, Yumoto H, Hirota K, *et al.* Histone-like DNA binding protein of Streptococcus intermedius induces the expression of pro-iflammatory cytokines in human monocytes via activation of ERK1/2 and JNK pathways. Cell Microbiol 2008;10:262–276.
30. Barak V, Selmi C, Schlesinger M, *et al.* Serum inflammatory cytokines, complements, and soluble interleukin 2 receptor in primary biliary cirrhosis. J Autoimmun 2009;33:178–182.
31. He XS, Ansari AA, Ridgway WM, *et al.* New insights to the immunopathology and autoimmune responses in primary biliary cirrhosis. Cell Immunol 2006;239:1–13.
32. Marsland BJ, Kopf M. Toll-like receptors: paving the path to T cell-driven autoimmunity? Curr Opin Immunol 2007;19: 611–614.